

Fast-weight Product Key Memory

Tianyu Zhao¹ and Llion Jones¹

¹Sakana AI

Sequence modeling layers in modern language models typically face a trade-off between storage capacity and computational efficiency. While Softmax attention offers unbounded storage at prohibitive quadratic costs, linear variants provide efficiency but suffer from limited, fixed-size storage. We propose Fast-weight Product Key Memory (FwPKM), a novel architecture that resolves this tension by transforming the sparse Product Key Memory (PKM) from a static module into a dynamic, “fast-weight” episodic memory. Unlike PKM, FwPKM updates its parameters dynamically at both training and inference time via local chunk-level gradient descent, allowing the model to rapidly memorize and retrieve new key-value pairs from input sequences. Experiments reveal that FwPKM functions as an effective episodic memory that complements the semantic memory of standard modules, yielding significant perplexity reductions on long-context datasets. Notably, in Needle in a Haystack evaluations, FwPKM generalizes to 128K-token contexts despite being trained on only 4K-token sequences.

Contents

1	Introduction	2
2	Product Key Memory	2
3	Fast-weight Product Key Memory	4
4	Experiments	9
5	Interpretability Analyses	11
6	Cost Analyses	15
7	Related Work	15
8	Conclusion	16
A	Detailed Training Settings	22
B	Ablation Study	23
C	More Visualization Examples	24

1. Introduction

Sequence modeling layers, or token mixers, are the foundational components in modern language models. The most successful architectures today can be fundamentally understood as forms of associative memory (Dao and Gu, 2024; Peng et al., 2025; Vaswani et al., 2017; Yang et al., 2024b, 2025), characterized by their ability to maintain key-value associations, execute retrieval, and perform memorization (Gershman et al., 2025).

Within this framework, existing layers lie on a spectrum defined by the trade-off between storage capacity and computational efficiency. Standard softmax attention (Vaswani et al., 2017) acts as an associative memory with unbounded storage, yet its computational cost becomes increasingly prohibitive as the sequence length grows (Zhong et al., 2025). Conversely, linear attention variants (Behrouz et al., 2025c; Dao and Gu, 2024; Gu and Dao, 2024; Katharopoulos et al., 2020; Schlag et al., 2021b; Sun et al., 2025; Yang et al., 2025) provide efficient, sub-quadratic mechanisms but rely on fixed storage capacities that often struggle to capture the same depth of information.

We focus our investigation on resolving this specific tension: balancing large-scale storage with low computational overhead. We posit that an ideal associative memory should satisfy four key properties:

1. Key-value Association: The ability to link keys to values.
2. Large Storage: Capacity that is extensive, if not unbounded.
3. Low Cost: Sub-quadratic computational complexity *w.r.t.* input length.
4. Retrieval and Memorization: The capability to retrieve information and, crucially, memorize new key-value pairs from inputs at any time.

Product Key Memory (PKM, Lample et al. 2019) is an architecture that elegantly satisfies the first three properties. Its sparse key-value design handles an enormous number of memory slots (e.g., $N = 10^6$) with fixed and low computation. However, PKM was originally designed as a “slow-weight” channel mixer – similar to Feed-Forward Networks (FFN) – meaning it is updated only during training and remains frozen during inference. Consequently, it lacks the ability to rapidly adapt to new inputs during deployment, failing property 4.

In this paper, we propose to convert PKM from a static, slow-weight module into Fast-weight Product Key Memory (FwPKM). By redesigning PKM to update its parameters dynamically at both training and inference time, we enable it to function as a high-fidelity episodic memory. FwPKM can store “episodes” directly from input sequences and carry that memory across different contexts, offering a promising new path for continual learning and personalized AI agents.

2. Product Key Memory

Top- k Key-value Memory A standard key-value memory consists of a key matrix $K \in \mathcal{R}^{N \times D_K}$ and a value matrix $V \in \mathcal{R}^{N \times D_V}$, where N represents the number of memory slots and $D_{\{K,V\}}$ are the hidden dimensions. A common approach to learning a large memory without sacrificing computation efficiency is to exploit sparsity via a Top- k operation (Rae et al., 2016; Weston et al., 2015). Given an input query vector \mathbf{q} , the model computes a score s_i for each memory slot as the inner product between the query and the keys. A Top- k operation \mathcal{T}_k then selects the indices of the k slots with the highest scores. The selected scores are normalized via softmax to produce weights $\{s'_i\}$, and the

Table 1 | Comparison of PKM and FwPKM

	PKM	FwPKM
Weight Type	Slow Weights	Fast Weights
Similar Modules	FFN, MoE-FFN, PKM	Softmax Attn., Linear Attn., DeltaNet
Role	Channel Mixer. Mixes features within a single token representation.	Token Mixer. Mixes information across time steps (sequence positions).
Parameter Update	Updated at training; Frozen at inference.	Updated at both training and inference.
Memory Horizon	Long-term (Semantic). Stores dataset-wide facts and general rules (e.g., world knowledge).	Short-term (Episodic). Stores context-specific variable bindings (the Context Window).
Learning Objective	Global Objective of next token prediction	Local Objective of memorization

retrieval output $\hat{\mathbf{v}}$ is computed as the weighted sum of the corresponding value slots.

$$s_i = \mathbf{q}^\top K_i \quad (1)$$

$$\mathcal{I} = \mathcal{T}_k(\mathbf{s}) \quad (2)$$

$$\{s'_i\} = \text{softmax}(\{s_j\}_{j \in \mathcal{I}}) \quad (3)$$

$$\hat{\mathbf{v}} = \sum_{i \in \mathcal{I}} V_i s'_i \quad (4)$$

Product Key Memory While the Top- k operation restricts the number of accessed memory slots, it still requires computing scores for all N key rows to find the top candidates. This $O(N)$ complexity prohibits scaling to enormous memory sizes (e.g. $N = 10^6$). Lample et al. (2019) proposed Product Key Memory (PKM) to address this problem. In PKM, the query vector \mathbf{q} is decomposed into two sub-queries \mathbf{q}^1 and \mathbf{q}^2 as shown below in Equation 5, where $[\cdot; \cdot]$ is concatenation. Instead of a single large key matrix, PKM maintains two smaller sub-key matrices $K^{\{1,2\}}$ each of size $\sqrt{N} \times D_K$. The memory slots are arranged in a Cartesian grid of size $\sqrt{N} \times \sqrt{N}$, and the slot at index (i, j) corresponds to the interaction between the i -th sub-key from K^1 and the j -th sub-key from K^2 . The score for this slot is defined as the sum of the scores of its corresponding sub-queries: $s_{(i,j)} = s_i^1 + s_j^2$. Importantly, under this formulation, the Top- k elements of this Cartesian product can be obtained without computing all N scores. Instead, it first identifies the Top- k indices for each sub-query independently and then searches within the smaller length- k^2 Cartesian product of these selected sets.

$$[\mathbf{q}^1; \mathbf{q}^2] = \mathbf{q} \quad (5)$$

$$s_i^{\{1,2\}} = \mathbf{q}^{\{1,2\}\top} K_i^{\{1,2\}} \quad (6)$$

$$\mathcal{I}^{\{1,2\}} = \mathcal{T}_k(\mathbf{s}^{\{1,2\}}) \quad (7)$$

$$\mathcal{I} = \mathcal{T}_k(\{s_i^1 + s_j^2 | i \in \mathcal{I}^1, j \in \mathcal{I}^2\}) \quad (8)$$

Once the final indices \mathcal{I} are selected, the remaining retrieval process (*i.e.* score normalization and weighted sum) keeps the same.

$$\hat{\mathbf{v}} = \text{PKM}(\mathbf{q}; K, V) = \sum_{i \in \mathcal{I}} V_i s'_i \quad (9)$$

The PKM architecture provides an elegant way to build a large-scale memory module at a low cost. A 10^6 -slot memory can be indexed using two small key matrices of size 10^3 , requiring only 2×10^3 score calculations. Furthermore, PKM naturally maintains a mapping between keys and values, thus making it an ideal foundation for the high-capacity associative memory we want to build.

3. Fast-weight Product Key Memory

The standard PKM is designed as a **slow-weight** channel mixer. In other words, its parameters are updated via a global objective (next-token prediction) over the entire training corpus but remain frozen during inference. Consequently, while it can store general semantic knowledge, it cannot adapt to new inputs or remember immediate contexts.

We propose to transform PKM into **Fast-weight PKM (FwPKM)**. We redesign the module to update its parameters dynamically at both training and inference time, by optimizing a local objective. This enables FwPKM to function as a high-fidelity episodic memory that captures key-value associations from the input stream itself.

3.1. Fast Weights

In standard neural networks, knowledge is stored in “slow weights” – parameters ϕ that are optimized over a massive training dataset but frozen after training. While effective for storing general knowledge in the dataset, slow weights lack the ability to rapidly adapt to new contexts. The concept of “fast weights” (Hinton and Plaut, 1987; Schmidhuber, 1992) addresses this problem by introducing a set of parameters that change dynamically according to every new input. The fast-weight parameters θ can be thought of as the storage of episodic memory.

Recent works like Test-Time Training (TTT, Sun et al. 2025) demonstrate that a fast-weight module can be implemented as a neural model $f(\cdot; \theta)$ and its parameters are updated by minimizing an MSE objective of an input sequence $\mathbf{h}_1, \dots, \mathbf{h}_T$. Formally, for an input \mathbf{h}_t in the sequence, the model performs a gradient descent step to minimize the MSE of reconstructing \mathbf{h}_t from its corrupted version $\tilde{\mathbf{h}}_t$ (e.g. via a low-rank projection):

$$\theta' = \theta - \eta \nabla_{\theta} \mathcal{L}_{\text{MSE}}(f(\tilde{\mathbf{h}}_t; \theta), \mathbf{h}_t) \quad (10)$$

$$= \theta - \eta \nabla_{\theta} \|\mathbf{h}_t - f(\tilde{\mathbf{h}}_t; \theta)\|_2^2, \quad (11)$$

where η is the learning rate. Through this optimization process, fast weights θ learn to encode information of the input sequence, at both training and inference time.

Following TTT, we implement fast weights by performing gradient descent updates on a local MSE objective during the forward pass. Specifically, we treat the key and value matrices as fast-weight parameters $\theta = \{K, V\}$. These parameters are updated via chunk-level gradient descent to minimize the reconstruction error of a chunk of query-value pairs.

Formally, for a chunk of size C , we generate query and target value inputs $\{(\mathbf{q}_t, \mathbf{v}_t)\}_{t=1}^C$ using slow-weight projections of the hidden states¹.

$$\mathbf{q}_t = \text{Linear}_{\phi}^q(\text{RMSNorm}_{\phi}^q(\mathbf{h}_t)) \quad (12)$$

$$\mathbf{v}_t = \text{Linear}_{\phi}^v(\text{RMSNorm}_{\phi}^v(\mathbf{h}_t)). \quad (13)$$

The model then computes a prediction $\hat{\mathbf{v}}_t$ using the current fast weights θ and updates it to minimize the Mean Square Error (MSE) between the prediction and target. We set the learning rate η to 1.0

¹We abuse the subscript of a tensor to index both the sequence dimension and the feature dimension(s). We use i, j to index the feature dimensions and t to index the sequence dimension.

and multiply the loss with a constant factor of 0.5.

$$\hat{\mathbf{v}}_t = \text{PKM}(\mathbf{q}_t; \theta) \quad (14)$$

$$\theta' = \theta - \sum_{t=1}^C \nabla_{\theta} \frac{1}{2} \mathcal{L}_{\text{MSE}}(\hat{\mathbf{v}}_t, \mathbf{v}_t). \quad (15)$$

3.2. Memorization Optimization

3.2.1. MSE loss

The optimization goal is to “rewrite” the memory such that retrieving with query \mathbf{q}_t yields the target value \mathbf{v}_t . We employ the Mean Squared Error (MSE) as our objective due to its favorable gradient properties for *explicit memory rewriting*.

The loss for a single sample is $\mathcal{L}_{\text{MSE}}(\hat{\mathbf{v}}, \mathbf{v}) = \frac{1}{2} \|\mathbf{v} - \hat{\mathbf{v}}\|_2^2$. Notably, we use a constant factor 0.5 and a learning rate of $\eta = 1.0$ as in Eq. 15. This is not arbitrary because it achieves the effect of “one-step rewriting”. The gradient *w.r.t.* the prediction $\hat{\mathbf{v}}$ is $\nabla_{\hat{\mathbf{v}}} \frac{1}{2} \mathcal{L}_{\text{MSE}}(\hat{\mathbf{v}}, \mathbf{v}) = -(\mathbf{v} - \hat{\mathbf{v}})$. A single gradient step therefore updates the prediction directly to the target.

$$\hat{\mathbf{v}}' = \hat{\mathbf{v}} - 1.0 \cdot (-(\mathbf{v} - \hat{\mathbf{v}})) = \mathbf{v}. \quad (16)$$

This allows FwPKM to instantly memorize the new key-value association.

In practice, we optimize the value matrix that produced the prediction, and the gradient *w.r.t.* the i -th value matrix row is instead given by

$$\nabla_{V_i} \frac{1}{2} \mathcal{L}_{\text{MSE}}(\hat{\mathbf{v}}, \mathbf{v}) = -(\mathbf{v} - \hat{\mathbf{v}}) s'_i. \quad (17)$$

3.2.2. Loss aggregation and gradient shaping

The last section showed the gradients for a single sample, but we process in chunks. As a result, a) an MSE loss will be calculated on every feature for every predicted value $\hat{\mathbf{v}}$ and b) multiple tokens may attempt to write the same value row simultaneously. In the following, we show the proper way to reduce the MSE losses in a chunk into a scalar loss for backpropagation and how to aggregate the gradients for a row in the value matrix.

Reducing MSE losses to a scalar by summation Instead of using averaging reduction, we reduce the MSE losses of a chunk of samples by summing over the sample and feature dimensions. Otherwise the gradient *w.r.t.* a value matrix element $V_{i,j}$ will be proportional to the actual update signal with a constant of $1/(\text{num_samples} \times D_V)$.

Weighting gradient by row contribution Let N_i^{read} be the “row contribution”, *i.e.* the number of times value row V_i is accessed within the current chunk. We scale the gradient for row i by $1/N_i^{\text{read}}$.

$$\nabla_{V_i}^{\text{agg}} = \frac{1}{N_i^{\text{read}}} \sum_{t=1}^C \nabla_{V_i} \frac{1}{2} \mathcal{L}_{\text{MSE}}(\hat{\mathbf{v}}_t, \mathbf{v}_t). \quad (18)$$

This averaging strategy acts as a consensus mechanism, ensuring that competitive memory writes from different tokens in the same chunk are balanced rather than accumulative.

Weighting MSE loss by token importance While the averaging strategy mitigates excessive memory writing, it treats all writings to the same slot equally. We weigh each MSE loss by a “gating value” g_t (defined in Section 3.4.4) to prioritize important updates within competitive writings. This scalar value represents the strength of FwPKM’s impact on the language model and the usefulness of its corresponding token.

No gradient clipping Unlike standard training, we explicitly avoid gradient clipping to fast-weight updates. Since the target values \mathbf{v} are unbounded, unclipped gradients are helpful for the memory to fully adapt to the scale of the target values.

3.3. Addressing Optimization

3.3.1. Marginal entropy loss

Sparse memory suffers from “memory collapsing” where the model learns to utilize only a small number of memory slots. [Lample et al. \(2019\)](#) showed that a vanilla PKM of $512 \times 512 = 262k$ slots can only reach 64.4% slot usage when selecting effectively Top-128 slots per token, with a multi-head mechanism where $4 \text{ heads} \times \text{Top-32 per head} = 128$ slots. The authors proposed applying batch normalization to queries and it raises the usage to 97.9%. However, we found the query normalization technique to become inefficient when the effective Top- k is small (e.g. 1 head with Top-8 slots per head), and a small effective Top- k is shown to be important for building a performant FwPKM (See ablation study in [Appendix B](#)).

We counteract FwPKM’s memory collapsing by optimizing an auxiliary addressing objective based on marginal entropy maximization. The goal is to encourage the model to access all memory slots uniformly on average across a chunk, without forcing a uniform distribution for any single individual query. Formally, for each of FwPKM’s sub key set, let $\mathbf{s}'_t \in \mathbb{R}^{\sqrt{N}}$ denote the normalized query-key scores after Top- k selection for token t in a chunk, where unselected indices have score 0. We compute the marginal distribution $\bar{\mathbf{p}}$ representing the average slot usage over the chunk and define the addressing loss as the marginal entropy of $\bar{\mathbf{p}} \in \mathbb{R}^{\sqrt{N}}$:

$$\bar{\mathbf{p}} = \frac{1}{C} \sum_{t=1}^C \mathbf{s}'_t \quad (19)$$

$$\mathcal{L}_{\text{addr}} = -H(\bar{\mathbf{p}}) = -\sum_{i=1}^{\sqrt{N}} \bar{p}_i \log \bar{p}_i. \quad (20)$$

While minimizing the MSE loss optimizes FwPKM’s value matrix V to store input values, minimizing the marginal entropy loss trains the key matrix K to adapt to input queries’ distribution, making the key vectors cover the query representation space more effectively and uniformly.

3.3.2. IDW score

A query-key score s_i in PKM is the dot product between a query and a key row $\mathbf{q}^\top K_i$. However, a key row can learn to change its magnitude to produce a larger score for a target query, without having to be “close” to the query in the representation space. Inverse distance weight (IDW, [McCarter 2023](#)) score is an alternative to dot-product score that produces a different key layout.

$$s_i^{\text{IDW}} = -\log(\epsilon + \|\mathbf{q} - K_i\|_2^2), \quad (21)$$

where $\epsilon = 10^{-3}$ following the paper. Due to the use of Euclidean distance, gradients produced by IDW scores will push keys to be “prototypes” – centroids of query clusters. We found that IDW score yields better performance than dot-product score.

3.4. Target Value Construction

3.4.1. Value residual

Target values are produced by a slow-weight network $\mathbf{v}_t = \text{Linear}_\phi^v(\text{RMSNorm}_\phi^v(\mathbf{h}_t))$. These slow-weight parameters, however, only directly participate in the computation of the fast-weight MSE loss whose gradients cannot reach slow weights. We add a residual connection from the output of the value projection layer to the output of FwPKM, so the value projection parameters are on the forward/backward path of the LM loss, which provides learning signals to make them produce target values that are useful for next token prediction.

3.4.2. Lookahead value

In a similar spirit to using short convolution in linear attention variants (Gu and Dao, 2024; Peng et al., 2023; Yang et al., 2024a), we pair queries with *lookahead* values when applying chunk-level updates. Essentially, we slightly modify the update rule in Eq. 15 by changing the timestep subscript of target value from t to $t + 1$. In this way, FwPKM associates each token’s key to its next token’s value, which provides more useful information for next token prediction.

$$\hat{\mathbf{v}}_{t+1} = \text{PKM}(\mathbf{q}_t; \theta) \quad (22)$$

3.4.3. Target value normalization

We also found it useful to z-score normalize target values on the feature dimension. Although the absence of grad clipping already ensures that value matrix V can adapt inputs of arbitrary scale, constraining the target values to have a mean of 0 and a standard deviation of 1 improves training stability.

3.4.4. Gating

Next token prediction does not always rely on episodic memory, so we devise a gating mechanism to give the model the freedom of determining how much information is extracted from FwPKM outputs. Similar to the computation of query and value vectors, we feed hidden state \mathbf{h}_t to an RMS normalization and a linear layer to compute a scalar value:

$$g_t = \text{Linear}_{\phi}^g(\text{RMSNorm}_{\phi}^g(\mathbf{h}_t)), \quad (23)$$

and the final output \mathbf{o}_t is an interpolation between the FwPKM output and the value residual:

$$\mathbf{o}_t = g_t \cdot \text{PKM}(\mathbf{q}_t; \theta) + (1 - g_t) \cdot \mathbf{v}_t \quad (24)$$

$$= g_t \cdot \hat{\mathbf{v}}_{t+1} + (1 - g_t) \cdot \mathbf{v}_t. \quad (25)$$

3.5. FwPKM Summary

We put everything together and show the complete formulation of FwPKM in the following and in Figure 1.

For each token t in a chunk, slow-weight network computes inputs to FwPKM.

$$\mathbf{q}_t, \mathbf{v}_t, g_t = \text{Linear}_{\phi}^{q,v,g}(\text{RMSNorm}_{\phi}^{q,v,g}(\mathbf{h}_t)) \quad (26)$$

FwPKM’s forward pass predicts the value at $t + 1$ from query at t , which is $\hat{\mathbf{v}}_{t+1} = \text{FwPKM}(\mathbf{q}_t; K^{\{1,2\}}, V)$. A step-by-step process is as follows. We omit timestep subscript t for variables other than the input \mathbf{q}_t and output $\hat{\mathbf{v}}_{t+1}$.

$$[\mathbf{q}^1; \mathbf{q}^2] = \mathbf{q} \quad (27)$$

$$s_i^{\{1,2\}} = -\log(\epsilon + \|\mathbf{q}^{\{1,2\}} - K_i^{\{1,2\}}\|_2^2) \quad (28)$$

$$\mathcal{I}^{\{1,2\}} = \mathcal{T}_k(\mathbf{s}^{\{1,2\}}) \quad (29)$$

$$\{s_i^{\{1,2\}}\}' = \text{softmax}(\{s_j^{\{1,2\}}\}_{j \in \mathcal{I}}) \quad (30)$$

$$\mathcal{I} = \mathcal{T}_k(\{s_i^1 + s_j^2 | i \in \mathcal{I}^1, j \in \mathcal{I}^2\}) \quad (31)$$

$$\hat{\mathbf{v}}_{t+1} = \sum_{i \in \mathcal{I}} V_i s_i' \quad (32)$$

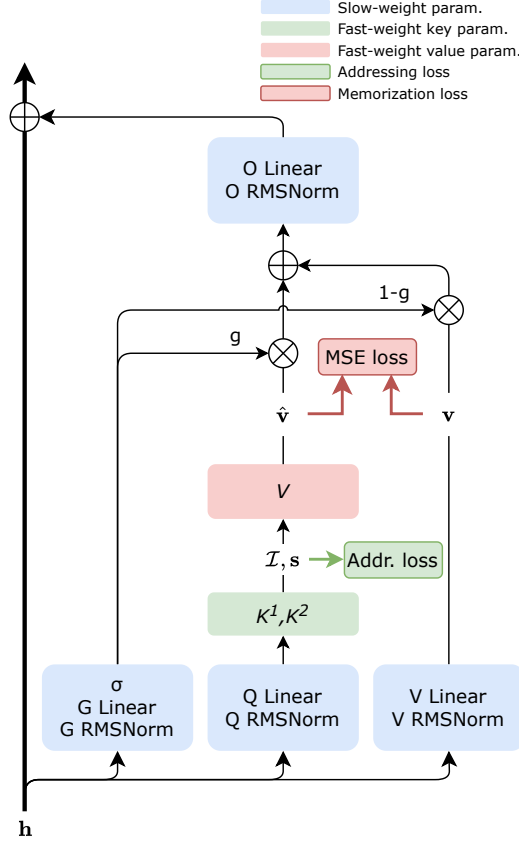


Figure 1 | Architecture of FwPKM.

The predicted value is combined with the value residual using the above gating value as weight. Lastly, an RMS normalization layer and a linear layer of slow weights are used to transform the output.

$$\mathbf{o}_t = g_t \cdot \hat{\mathbf{v}}_{t+1} + (1 - g_t) \cdot \mathbf{v}_t \quad (33)$$

$$\mathbf{o}'_t = \text{Linear}_\phi^o(\text{RMSNorm}_\phi^o(\mathbf{o}_t)) \quad (34)$$

Once we have collected the predicted values and target values for a chunk, we apply an update to the FwPKM's parameters $\theta = \{V, K^1, K^2\}$. The value matrix is updated using shaped gradients from the MSE losses weighted by gating values.

$$\nabla_{V_i}^{\text{agg}} = \frac{1}{N_i^{\text{read}}} \sum_{t=1}^C \nabla_{V_i} \frac{1}{2} g_t \mathcal{L}_{\text{MSE}}(\hat{\mathbf{v}}_t, \mathbf{v}_t) \quad (35)$$

$$V'_i = V_i - \nabla_{V_i}^{\text{agg}}. \quad (36)$$

The key matrices are updated using gradients from the marginal entropy-based addressing loss.

$$\bar{\mathbf{p}} = \frac{1}{C} \sum_{t=1}^C \mathbf{s}'_t \quad (37)$$

$$\mathcal{L}_{\text{addr}} = - \sum_{i=1}^{\sqrt{N}} \bar{p}_i \log \bar{p}_i \quad (38)$$

$$K' = K - \nabla_K \mathcal{L}_{\text{addr}}, \quad K \in \{K^1, K^2\} \quad (39)$$

4. Experiments

4.1. Training Setting

Model We implement language models based on the QwenNext architecture², which interleaves Gated DeltaNet (GDN, Yang et al., 2025) and gated softmax attention layers (Qiu et al., 2025). Our investigation uses these 12-layer baseline configurations.

- GDN: Gated DeltaNets at all 12 layers
- GDN+SWA: GDN interleaved with Sliding Window Attention (SWA, window size 512) at a 3:1 ratio
- GDN+FA: GDN interleaved with Full Attention (FA) at a 3:1 ratio
- FA: Full Attention at all layers

We introduce PKM and FwPKM modules into these baselines at specific depths (layers 2, 6, and 10). A standard PKM layer replaces the original FFN, while an FwPKM layer is inserted between the token mixer (Attention/GDN) and the FFN. Both PKM and FwPKM have 512^2 memory slots. PKM retrieves effectively Top-128 slots (4 heads and 32 slots per head) while FwPKM retrieves Top-8 slots (1 head and 8 slots per head).

We further include two types of baselines. For the first kind, we substitute the PKM architecture in FwPKM@2, 6, 10 with a SwiGLU MLP (Shazeer, 2020) that maintains three fast-weight matrices and their biases for up-/gating-/down-projection. This variant is denoted as FwMLP@2, 6, 10. In addition, we use LaCT (Zhang et al., 2025b) as the second baseline. LaCT is an improved TTT (Sun et al., 2025) model that uses a sliding window attention, a fast-weight SwiGLU MLP, and a slow-weight SwiGLU MLP in every layer. Its fast weights are updated using SGD+momentum with L2 weight normalization (Salimans and Kingma, 2016).

Data To incentivize the learning of cross-chunk dependencies via FwPKM, we use 5B tokens from LongContext64 (Buckman), a dataset consisting of long-context documents ($> 64K$ tokens) sourced from RedPajama V2 (Weber et al., 2024). We supplement this with 5B tokens from Fineweb-Edu (Penedo et al., 2024) to maintain high-quality language modeling capabilities. All models are trained with a sequence length of 4K tokens.

We refer readers to Appendix A for more details of the architectures and optimization.

4.2. PPL Evaluation

We evaluate perplexity (PPL) on three distinct datasets to assess different memory capabilities: **Fineweb-Edu** (knowledge-intensive, short context), **LC64** (in-domain, long context), and **LAMBADA** (Paperno et al. 2016, out-of-domain, long context). Each evaluation dataset contains 8M tokens. We evaluate 4K-token sequences in their original order with a batch size of 1 so that sequences from the same document are presented sequentially. This enables fast weights to capture the dependency between adjacent sequences. Figure 2 shows the perplexities on the datasets for all models.

Finding 1: FwPKM and PKM serve distinct, complementary roles Baseline models with layouts GDN and GDN+SWA lack components for modeling long-range dependency, and their FwPKM versions address the weakness. As shown in Figure 2, FwPKM significantly reduces PPL on long-context datasets (LC64, LAMBADA), confirming its role as an **episodic memory**. In contrast, standard PKM provides the largest gains on Fineweb-Edu, acting as a **semantic memory** for global knowledge. The combination of both modules yields the best performance across all metrics, suggesting they address orthogonal limitations in the baseline architectures.

²<https://huggingface.co/Qwen/Qwen3-Next-80B-A3B-Thinking>

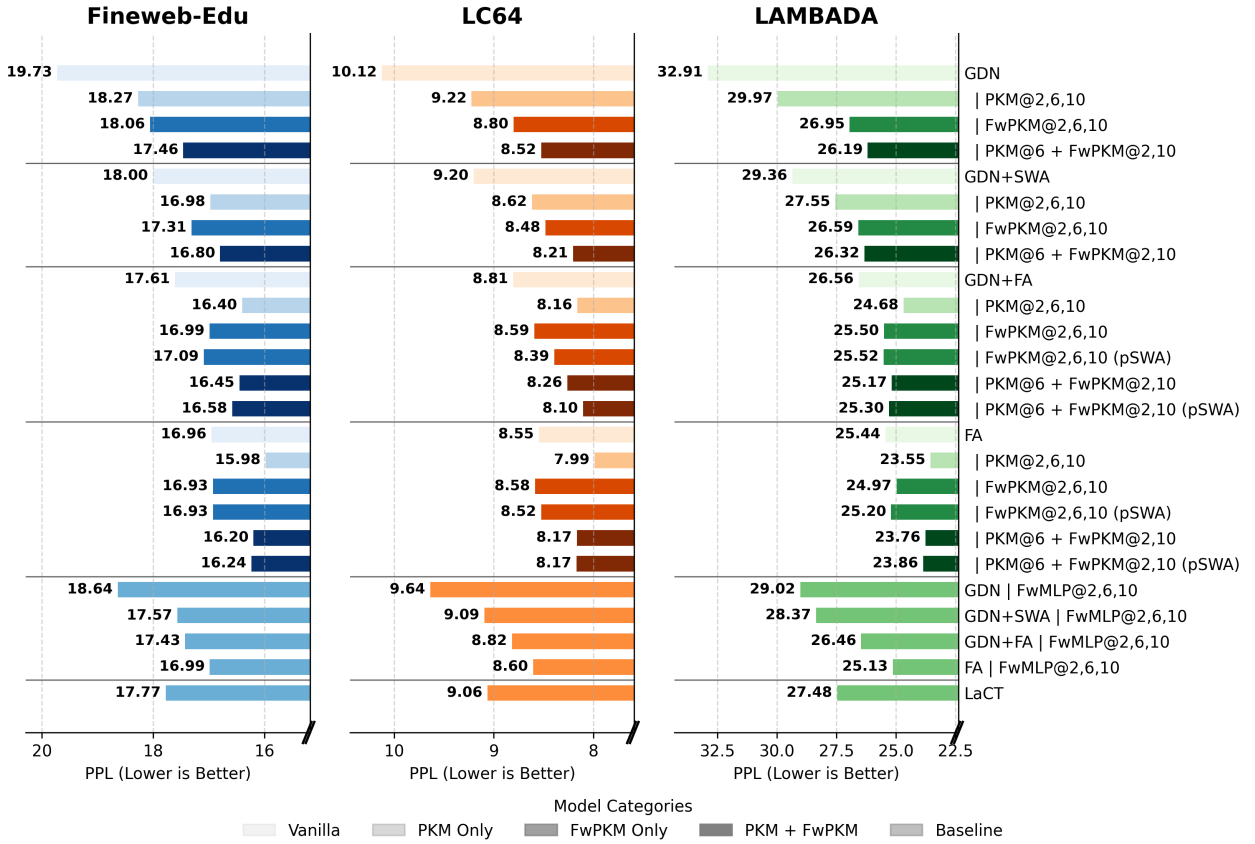


Figure 2 | Perplexity on Fineweb-Edu, LC64, and LAMBADA

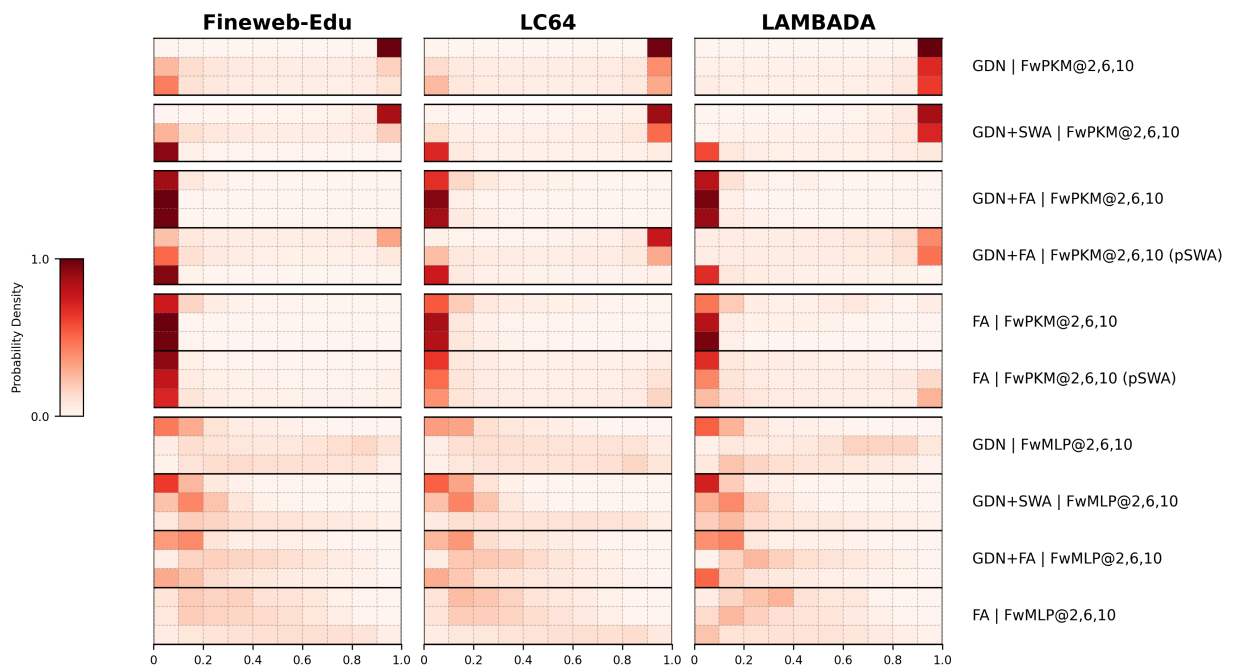


Figure 3 | FwPKM gating value distribution on Fineweb-Edu, LC64, and LAMBADA test sets. Each row represents one FwPKM layer.

Finding 2: FwPKM competes with Full Attention When FwPKM is added to baselines with unrestricted Full Attention (FA and GDN+FA), PPL improvements are marginal. Analysis of gating values in Figure 3 reveals that these models learn to ignore FwPKM, with gating weights clustering near zero.

Finding 3: Restricting full attention facilitates FwPKM use. To mitigate the above issue, we restrict full attention’s long-range perception at training time, by imposing a sliding attention window of length 512 to all full attentions with a probability of 0.9. Denoted by a suffix pSWA, these new models learn to use FwPKM more as suggested by more gating value distribution mass on the high-value end in Figure 3. While pSWA has minimal impact in the PPL evaluation, we will see a more significant difference in the following section.

4.3. NIAH Evaluation

We conduct Needle in a Haystack (NIAH, [Kamradt 2023](#); [Mohtashami and Jaggi 2023](#)) evaluation to further verify FwPKM’s functionality as episodic memory.

In the basic setting, we construct 500 NIAH samples from the LAMBADA dataset. Each sample contains a haystack – a 4K-length sequence from the LAMBADA dataset with 5 needles inserted at random positions, where each needle contains a unique 4-character key and a 6-digit value – and a question that requests the value of a specific key. To test FwPKM’s large memory storage, we additionally construct test sets of 8K, 32K, and 128K context lengths.

Iterative Memorization (n -iter NIAH) A unique feature of FwPKM is its ability to improve memory fidelity by re-processing the same input. We define a n -iter NIAH setting, where the model forwards the same haystack context n times before answering. FwPKM’s process chunk size C is accordingly changed to the length of each haystack context such that it updates its memory once after reading an entire haystack. The basic setting is 1-iter NIAH.

Accuracy results of n -iter NIAH ($n \in \{1, 2, 3, 4\}$) on the four test sets of 4K-128K context lengths are shown in Figure 4. The accuracies of all iterations are drawn as a stacked bar.

Finding 4: Iterative reading boosts retrieval accuracy. For GDN and GDN+SWA layouts, a single pass (1-iter) is often insufficient for perfect retrieval. However, a second pass (2-iter) yields a massive boost in accuracy (jumping from $< 10\%$ to $> 70\%$ in many cases). This confirms that FwPKM effectively exploits test-time training to consolidate episodic memories, surpassing softmax attention. In addition, effective iterative memorization (in Figure 4) correlates with high gating values (in Figure 3).

Finding 5: FwPKM generalizes to 128K contexts. Despite being trained on only 4K-token sequences, FwPKM generalizes effectively to 128K tokens. While FA baselines degrade rapidly on context lengths unseen during training, FwPKM maintains robust retrieval performance.

Finding 6: Longer context requires more memorization iterations. As context length grows from 4K to 128K, the 2-iter accuracy significantly reduces from $> 70\%$ to 40% for GDN + FwPKM@2,10 and more severely for other models. However, more iterations largely fill in the gap.

5. Interpretability Analyses

A key advantage of FwPKM over black-box architectures is its inherent interpretability. Because memory slots are explicitly written and read, we can trace retrieved information back to specific input tokens.

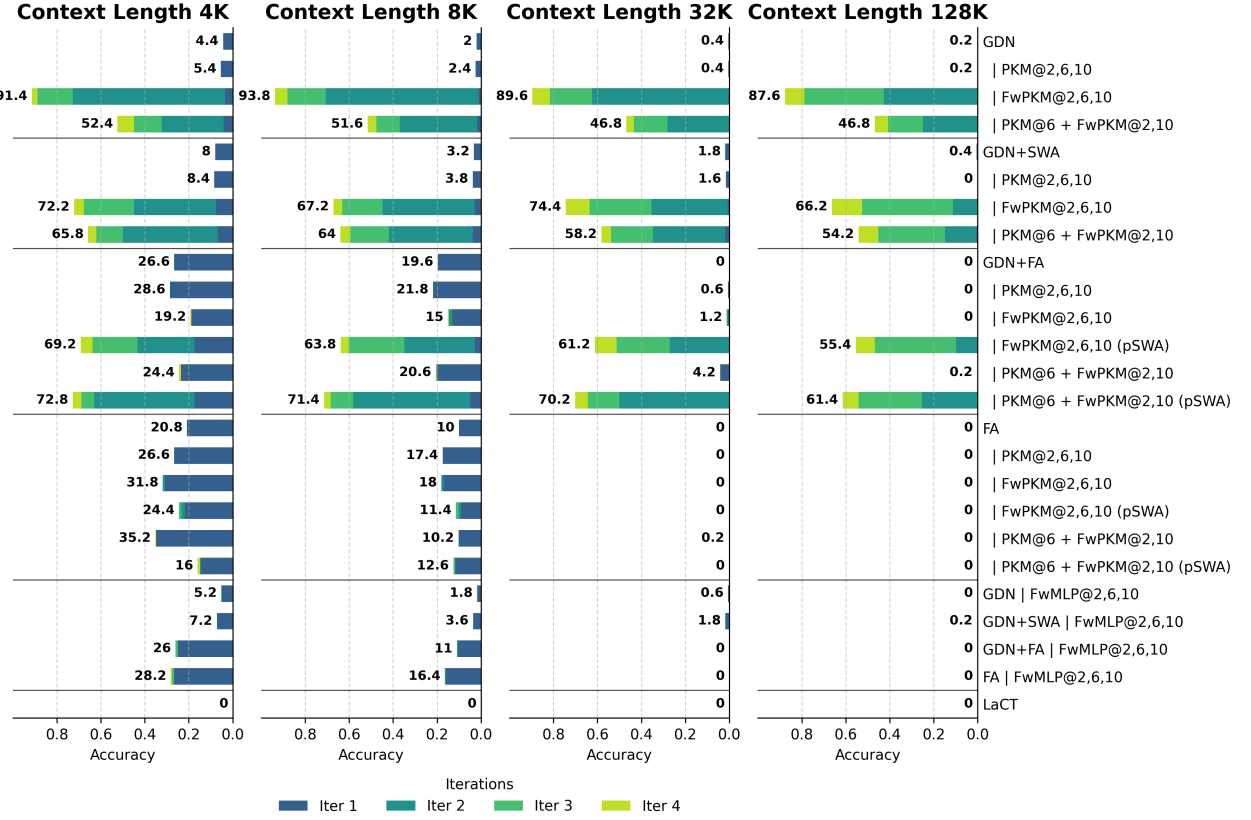


Figure 4 | Stacked bar plots for NIAH accuracy results on 4K-/8K-/32K-/128K-length test sets. Each stacked bar shows the accuracies of {1, 2, 3, 4}-iter NIAH evaluations.

5.1. Case Study: Probing Memory in NIAH

We analyze the memory access patterns of the GDN+PKM@6+FwPKM@2,10 model during the 4-iter NIAH task (4K context). At each generation step, every memory layer returns Top-8 retrieved slots. We show the content stored in each slot from the latest memorization³, namely the **query token**, the **target value token**, and its surrounding context. In addition, a **[HIT]** label indicates whether a slot stores the ground-truth next token.

High-precision retrieval As shown in Figure 5, the majority of retrieved slots contain the correct target tokens associated with the query needle.

Error analysis Incorrect retrievals typically share the same query token as the input but lack the correct prefix context. This suggests that retrieval errors stem from imperfect prefix matching in the latent query space rather than storage failure.

Robust aggregation Despite the slot errors, the model successfully aggregates information across the 16 slots from 2 FwPKM layers to generate the correct 6-digit value, demonstrating robust distributed storage.

³A slot may contain information from earlier updates, but we omit them due to space limit.

Needles

... ID-1b22: 385738 ... [TARGET] ID-f2de: 777143 ... ID-0a98: 045247 ... ID-5224: 555194 ... ID-4884: 543884 ...

Output Token 1: '7'

--- FwPKM Layer 2 ---

Slot 196281 | | Q: | V in ctx:...D-1b22 is 385738. had...
 Slot 67257 | | Q: | V in ctx:...D-1b22 is 385738. had...
 Slot 196567 | | Q: | V in ctx:...D-1b22 is 385738. had...
 Slot 196126 | [HIT] | Q: | V in ctx:...D-f2de is 777143. and...
 Slot 196273 | [HIT] | Q: | V in ctx:...D-f2de is 777143. and...
 Slot 196510 | | Q: | V in ctx:...D-1b22 is 385738. had...
 Slot 67543 | | Q: | V in ctx:...D-1b22 is 385738. had...
 Slot 196513 | [HIT] | Q: | V in ctx:...D-f2de is 777143. and...

--- FwPKM Layer 10 ---

Slot 13369 | | (Empty)
 Slot 63545 | | (Empty)
 Slot 13803 | [HIT] | Q: | V in ctx:...D-f2de is 777143. and...
 Slot 13378 | | Q:ed | V in ctx:...s littered with straw and...
 Slot 65081 | | Q:ling | V in ctx:...d bustling , infused w...
 Slot 224825 | [HIT] | Q: | V in ctx:...D-f2de is 777143. and...
 Slot 57 | | Q: | V in ctx:...D-0a98 is 045247. eve...
 Slot 7737 | | Q:en | V in ctx:...mujahedeen , taking an...

Output Token 2: '7'

--- FwPKM Layer 2 ---

Slot 61131 | [HIT] | Q:7 | V in ctx:...-f2de is 777143. and ...
 Slot 61214 | [HIT] | Q:7 | V in ctx:...-f2de is 777143. and ...
 Slot 61397 | | Q: eight | V in ctx:...ns , eight hours had gone ...
 Slot 61287 | (Empty)
 Slot 54475 | | Q:7 | V in ctx:...-lc66 is 752940. push...
 Slot 114891 | [HIT] | Q:7 | V in ctx:...-f2de is 777143. and ...
 Slot 80587 | (Empty)
 Slot 61102 | (Empty)

--- FwPKM Layer 10 ---

Slot 63862 | | Q: | V in ctx:... 28 fiery 29 turquoise...
 Slot 63545 | | (Empty)
 Slot 103798 | | Q: was | V in ctx:...k eyes was evident , and war...
 Slot 36214 | (Empty)
 Slot 16758 | (Empty)
 Slot 103481 | (Empty)
 Slot 35897 | | Q:6 | V in ctx:... 69603dark fo...
 Slot 16441 | | Q: war | V in ctx:...ont of wara 's table ...

Output Token 3: '7'

--- FwPKM Layer 2 ---

Slot 94396 | [HIT] | Q:7 | V in ctx:...f2de is 777143. and t...
 Slot 94710 | | Q:7 | V in ctx:...2de is 777143. and th...
 Slot 94366 | [HIT] | Q:7 | V in ctx:...f2de is 777143. and t...
 Slot 94346 | [HIT] | Q:7 | V in ctx:...f2de is 777143. and t...
 Slot 94481 | [HIT] | Q:7 | V in ctx:...f2de is 777143. and t...
 Slot 94460 | [HIT] | Q:7 | V in ctx:...f2de is 777143. and t...
 Slot 94464 | [HIT] | Q:7 | V in ctx:...f2de is 777143. and t...
 Slot 94418 | [HIT] | Q:7 | V in ctx:...f2de is 777143. and t...

--- FwPKM Layer 10 ---

Slot 125284 | [HIT] | Q:7 | V in ctx:...f2de is 777143. and t...
 Slot 125347 | [HIT] | Q:7 | V in ctx:...f2de is 777143. and t...
 Slot 63844 | | Q: his | V in ctx:...ripped his arms tightly b...
 Slot 210788 | [HIT] | Q:7 | V in ctx:...f2de is 777143. and t...
 Slot 125225 | [HIT] | Q:7 | V in ctx:...f2de is 777143. and t...
 Slot 125187 | [HIT] | Q:7 | V in ctx:...f2de is 777143. and t...
 Slot 63907 | [HIT] | Q:7 | V in ctx:...-f2de is 777143. and ...
 Slot 210851 | (Empty)

Output Token 4: '1'

--- FwPKM Layer 2 ---

Slot 94411 | [HIT] | Q:7 | V in ctx:...2de is 777143. and th...
 Slot 3275 | [HIT] | Q:7 | V in ctx:...2de is 777143. and th...
 Slot 10443 | [HIT] | Q:7 | V in ctx:...2de is 777143. and th...
 Slot 94710 | [HIT] | Q:7 | V in ctx:...2de is 777143. and th...
 Slot 94291 | [HIT] | Q:7 | V in ctx:...2de is 777143. and th...
 Slot 94709 | [HIT] | Q:7 | V in ctx:...2de is 777143. and th...
 Slot 94512 | | Q:7 | V in ctx:...22 is 385738. had let...
 Slot 94396 | | Q:7 | V in ctx:...f2de is 777143. and t...

--- FwPKM Layer 10 ---

Slot 16009 | [HIT] | Q:7 | V in ctx:...2de is 777143. and th...
 Slot 15933 | [HIT] | Q:7 | V in ctx:...2de is 777143. and th...
 Slot 15926 | | Q: asked | V in ctx:...ever asked . `` i can ...
 Slot 16259 | (Empty)
 Slot 16037 | | Q:qu | V in ctx:...ant a taqui a. `` she...
 Slot 112777 | [HIT] | Q:7 | V in ctx:...2de is 777143. and th...
 Slot 214153 | [HIT] | Q:7 | V in ctx:...2de is 777143. and th...
 Slot 16081 | | Q: rewar | V in ctx:...uld reward him with eter...

Output Token 5: '4'

--- FwPKM Layer 2 ---

Slot 105998 | [HIT] | Q:1 | V in ctx:...de is 777143. and the...
 Slot 106436 | [HIT] | Q:1 | V in ctx:...de is 777143. and the...
 Slot 106414 | [HIT] | Q:1 | V in ctx:...de is 777143. and the...
 Slot 106286 | [HIT] | Q:1 | V in ctx:...de is 777143. and the...
 Slot 18958 | [HIT] | Q:1 | V in ctx:...de is 777143. and the...
 Slot 19396 | [HIT] | Q:1 | V in ctx:...de is 777143. and the...
 Slot 210958 | [HIT] | Q:1 | V in ctx:...de is 777143. and the...
 Slot 211396 | (Empty)

--- FwPKM Layer 10 ---

Slot 168289 | | Q: a | V in ctx:...lowed by a short little do...
 Slot 168086 | | Q: comfo | V in ctx:...be comforting , was n't...
 Slot 109409 | [HIT] | Q:1 | V in ctx:...de is 777143. and the...
 Slot 109206 | | Q:7 | V in ctx:...2de is 777143. and th...
 Slot 168304 | | Q: tenni | V in ctx:...rse tennis shoe through t...
 Slot 148833 | [HIT] | Q:1 | V in ctx:...de is 777143. and the...
 Slot 148630 | | Q:2 | V in ctx:...98 is 045247. everyon...
 Slot 96097 | | Q: a | V in ctx:... towards a larger , low-slu...

Output Token 6: '3'

--- FwPKM Layer 2 ---

Slot 216065 | [HIT] | Q:4 | V in ctx:...e is 777143. and then...
 Slot 216364 | [HIT] | Q:4 | V in ctx:...e is 777143. and then...
 Slot 9729 | [HIT] | Q:4 | V in ctx:...e is 777143. and then...
 Slot 208385 | [HIT] | Q:4 | V in ctx:...e is 777143. and then...
 Slot 10028 | [HIT] | Q:4 | V in ctx:...e is 777143. and then...
 Slot 208684 | [HIT] | Q:4 | V in ctx:...e is 777143. and then...
 Slot 139777 | [HIT] | Q:4 | V in ctx:...e is 777143. and then...
 Slot 216073 | | Q:4 | V in ctx:...e is 777143. and then...

--- FwPKM Layer 10 ---

Slot 169986 | | Q:0 | V in ctx:... 69603dark form ...
 Slot 170045 | | Q:7 | V in ctx:...22 is 385738. had let...
 Slot 170465 | [HIT] | Q:4 | V in ctx:...e is 777143. and then...
 Slot 170472 | [HIT] | Q:4 | V in ctx:...e is 777143. and then...
 Slot 170077 | [HIT] | Q:4 | V in ctx:...e is 777143. and then...
 Slot 170121 | | Q:7 | V in ctx:...22 is 385738. had let...
 Slot 97282 | | Q: t | V in ctx:...me green t-shirts at ...
 Slot 97341 | | Q:1 | V in ctx:...f00 is 221391. one he...

Figure 5 | An example of FwPKM slot access of GDN+PKM@6+FwPKM@2,10 during generating an NIAH-4K answer. The model memorizes the haystack for 3 extra iterations, i.e. 4-iter NIAH.

Figure 6 | GDN+PKM@6+FwPKM@2, 10's FwPKM gating values on tokens from the Wikipedia article for Sakana AI.

5.2. Case Study: Selective Gating

We further examine the “gating values” g_t to understand when the model chooses to rely on episodic memory versus its static slow weights. Using the Wikipedia article for “Sakana AI”⁴ as a test case, we change the model’s update chunk size from 512 to 32 to adapt for the article’s length. As shown in Figure 6, we can observe distinct behaviors across layers.

Layer specialization The lower-layer FwPKM tends to maintain high gating values across all tokens, serving as a general-purpose buffer. In contrast, the higher-layer FwPKM exhibits highly selective activation.

Novelty detection In the higher layer, gating values spike specifically for tokens related to rare named entities (e.g. “Sakana AI”, “David Ha”, “Llion Jones”, and “Ren Ito”). This indicates that the model effectively distinguishes between general linguistic patterns and novel, context-specific entities, which are processed by slow weights and fast weights, respectively.

⁴https://en.wikipedia.org/wiki/Sakana_AI

Table 2 | Comparison of model size and computation cost.

MODEL	Parameters (M)	FLOPs (T)	FLOPS (T/sec.)	Samples/sec.
GDN	112.11	22.05	121.82	42.81
PKM@2,6,10	509.08	20.91	84.47	30.09
FwPKM@2,6,10	519.12	22.74	46.44	16.10
PKM@6 + FwPKM@2,10	515.77	22.14	54.63	19.26
GDN+SWA	112.65	22.14	124.42	43.45
PKM@2,6,10	509.61	21.03	88.16	31.25
FwPKM@2,6,10	519.66	22.86	47.16	16.27
PKM@6 + FwPKM@2,10	516.31	22.23	55.30	19.39
GDN+FA	112.65	22.14	120.67	42.08
PKM@2,6,10	509.61	21.03	84.69	30.07
FwPKM@2,6,10	519.66	22.86	46.51	16.05
PKM@6 + FwPKM@2,10	516.31	22.23	54.99	19.29
FA	114.25	22.47	120.45	41.55
PKM@2,6,10	511.22	21.33	81.22	28.49
FwPKM@2,6,10	521.26	23.16	46.63	15.89
PKM@6 + FwPKM@2,10	517.91	22.56	54.43	18.84

6. Cost Analyses

We compare the main models' parameter numbers and computation costs in Table 2. In particular, we report **FLOPs** (Floating Point Operations) to measure the required computation as well as **FLOPS** (Floating Point Operations Per Second), which is FLOPs divided by running time (in seconds), to additionally take into account implementation efficiency.

The sparsity of PKM/FwPKM makes it even less FLOPs-intensive than a baseline MLP layer despite much increased model size. However FLOPS numbers suggest that PKM/FwPKM components take longer to run. One main reason is the large gap between their efficient implementation. Softmax attention and linear attention (e.g. GDN) are fast using kernels from FlashAttention (Dao, 2024; Dao et al., 2022) and FlashLinearAttention (Yang and Zhang, 2024). An important future direction for this work is to design more efficient kernels to facilitate easier scaling up and a broader adoption of the FwPKM model.

7. Related Work

Softmax attention and linear variants Standard softmax attention has been foundational to the success of Transformers (Vaswani et al., 2017), fundamentally acting as a powerful form of associative memory (Zhong et al., 2025). However, its quadratic complexity limits its application to extremely long sequences. To address this, various efficient architectures have been proposed. Linear attention (Katharopoulos et al., 2020) reduces complexity to linear time by changing the order of association. This direction includes Recurrent Neural Network (RNN) and State Space Model (SSM) evolutions such as Mamba (Gu and Dao, 2024) and Mamba2 (Dao and Gu, 2024), as well as specific variants like DeltaNet (Schlag et al., 2021b; Yang et al., 2024b), Gated DeltaNet (Yang et al., 2025), and RWKV7 (Peng et al., 2025). Other approaches like Memory Mosaics (Zhang and Bottou, 2025; Zhang et al., 2025a) improve softmax attention by techniques such as time-dimension smoothing and hierarchical memory design.

Fast weights and test-time training The concept of “fast weights” offers a powerful lens for unifying sequence modeling. Rooted in early work by Schmidhuber (1992) and Ba et al. (2016), this

framework views linear transformers as fast weight programmers (Schlag et al., 2021a). Recently, this paradigm has been revitalized by Test-Time Training (TTT) (Sun et al., 2025; Zhang et al., 2025b) and Titans (Behrouz et al., 2025c), which explicitly update parameters during inference using gradient descent, enabling the model to memorize the current context. Theoretical frameworks like MIRAS (Behrouz et al., 2025a) and Test-Time Regression (Wang et al., 2025) unified various sequence models under the umbrella of test-time optimization and associative memory. These frameworks pointed out several directions for new model designs, namely memory architecture, memorization rule, memory retention rule, and optimizer. Our proposal of FwPKM contributes a novel memory architecture and a specific memorization rule accommodated for its structural sparsity.

Hybrid architectures Recognizing the complementary strengths of different sequence models, recent work has increasingly focused on hybrid architectures that combine the high-fidelity retrieval of quadratic attention with the efficiency of linear or recurrent layers. This includes hybrid models trained from scratch (Irie et al., 2025), as well as large-scale Hybrid LLMs such as Samba (Ren et al., 2025) and KimiLinear (Team et al., 2025). QwenNext also employs this interleaved design. Furthermore, approaches like Artificial Hippocampus Networks (AHN, Fang et al. 2025) explore fine-tuning techniques to integrate these distinct memory systems effectively. Experiments in Section 4 demonstrated interactions between memories of different characteristics. The combination of linear attention (*i.e.* GDN), softmax attention, slow-weight sparse memory (*i.e.* PKM), and fast-weight sparse memory (*i.e.* FwPKM) implements a versatile memory system that excels at various tasks.

Memory models Beyond implicit knowledge in weights, explicit memory modules have been explored to enhance storage capacity. Early works include Memory Networks (Weston et al., 2015), while recent studies suggest even simple MLPs can function as memory (Csordás et al., 2023). To scale up capacity without prohibitive costs, sparse access mechanisms are essential. Product Key Memory (PKM, Berges et al. 2025; Lample et al. 2019) and PEER (He, 2024) utilize sparsity to access massive memory banks efficiently. Ultra Sparse Memory (Huang et al., 2025a,b) is a line of work that extends the PKM architecture with more expressive keys and other improvements. Our work builds upon the PKM structure but transitions it from a static “slow” memory to a dynamic “fast” memory.

Continual and episodic learning Finally, the ability to update memory parameters allows for continual learning and adaptation. Lin et al. (2025) showed that parameter-efficient fine-tuning of PKM effectively mitigates catastrophic forgetting. It demonstrated one dimension for continual learning – optimizing sparse slow weights via self-supervised learning to update semantic memory. FwPKM opens up the possibility for a different dimension of updating episodic memory by learning fast weights in an online learning manner. Nested Learning (Behrouz et al., 2025b) and TNT (Li et al., 2025) explored the direction of stacking multiple fast weight layers (*e.g.* Titans) and apply memory updates at varying frequencies. This “nested” memory structure enables gradually digesting changes in faster weights into slower weights and exhibits strong performance. FwPKM maintains a huge memory bank and is updated at a low frequency to amortize optimization cost. It is a promising direction to design a hybrid memory system of varying-size FwPKMs and other memory components such as Titans with different optimization strategies as in Nested Learning (Behrouz et al., 2025b).

8. Conclusion

In this work, we introduced **Fast-weight Product Key Memory (FwPKM)**, a memory-augmented layer that unifies PKM’s large-scale sparse storage with the rapid adaptability of fast weights. Concretely, FwPKM extends Product Key Memory from a static retrieval module into a context-responsive component whose parameters can be updated online, allowing the model to write information into memory and later retrieve it. This addresses a key limitation of prior sparse memory modules, namely their inability to efficiently incorporate new evidence at inference time, and makes PKM better

suited for long-context settings where relevant information may be separated by many thousands of tokens.

Empirically, we find that FwPKM remains effective far beyond its training regime. Models trained on 4K-token sequences generalize to 128K-token contexts, while exhibiting behavior consistent with a robust episodic memory that complements the semantic knowledge stored in standard layers.

At the same time, several challenges remain. Online updates introduce additional computation and choices such as chunk size, update frequency, and optimization hyperparameters. Scaling these updates efficiently motivates further systems work, including faster sparse update kernels and better implementation strategies. On the modeling side, future works include more powerful and robust memory design regarding its architecture, update rule, and retention. Overall, by integrating sparse storage with fast, context-driven updates, FwPKM offers a promising step toward language models with versatile and mutually complementary memory components.

Acknowledgments

We thank Kai Arulkumaran, Luke Darlow, Stefania Druga and the rest of the Sakana AI team for fruitful discussions throughout the project.

References

Jimmy Ba, Geoffrey E. Hinton, Volodymyr Mnih, Joel Z. Leibo, and Catalin Ionescu. Using fast weights to attend to the recent past. In *NeurIPS*, 2016.

Ali Behrouz, Meisam Razaviyayn, Peilin Zhong, and Vahab Mirrokni. It's all connected: A journey through test-time memorization, attentional bias, retention, and online optimization, 2025a. URL <https://arxiv.org/abs/2504.13173>.

Ali Behrouz, Meisam Razaviyayn, Peilin Zhong, and Vahab Mirrokni. Nested learning: The illusion of deep learning architectures. In *NeurIPS*, 2025b. URL <https://openreview.net/forum?id=nbMeRvNb7A>.

Ali Behrouz, Peilin Zhong, and Vahab Mirrokni. Titans: Learning to memorize at test time. In *NeurIPS*, 2025c. URL <https://openreview.net/forum?id=8GjSf9Rh7Z>.

Vincent-Pierre Berges, Barlas Oguz, Daniel Haziza, Wen-tau Yih, Luke Zettlemoyer, and Gargi Ghosh. Memory layers at scale. In *ICML*, 2025.

Jacob Buckman. Longcrawl64: A Long-Context Natural-Language Dataset.

Róbert Csordás, Kazuki Irie, and Jürgen Schmidhuber. Approximating two-layer feedforward networks for efficient transformers. In *Findings of EMNLP*. Association for Computational Linguistics, 2023.

Tri Dao. FlashAttention-2: Faster attention with better parallelism and work partitioning. In *ICLR*, 2024.

Tri Dao and Albert Gu. Transformers are ssms: Generalized models and efficient algorithms through structured state space duality. In *ICML*, 2024.

Tri Dao, Daniel Y. Fu, Stefano Ermon, Atri Rudra, and Christopher Ré. FlashAttention: Fast and memory-efficient exact attention with IO-awareness. In *NeurIPS*, 2022.

Yunhao Fang, Weihao Yu, Shu Zhong, Qinghao Ye, Xuehan Xiong, and Lai Wei. Artificial hippocampus networks for efficient long-context modeling, 2025. URL <https://arxiv.org/abs/2510.07318>.

Samuel J. Gershman, Ila Fiete, and Kazuki Irie. Key-value memory in the brain. *Neuron*, 113(11): 1694–1707.e1, 2025. ISSN 0896-6273.

Albert Gu and Tri Dao. Mamba: Linear-time sequence modeling with selective state spaces. In *COLM*, 2024. URL <https://openreview.net/forum?id=tEYskw1VY2>.

Xu Owen He. Mixture of a million experts, 2024. URL <https://arxiv.org/abs/2407.04153>.

Geoffrey E Hinton and David C Plaut. Using fast weights to deblur old memories. In *Proceedings of the ninth annual conference of the Cognitive Science Society*, pages 177–186, 1987.

Zihao Huang, Yu Bao, Qiyang Min, Siyan Chen, Ran Guo, Hongzhi Huang, Defa Zhu, Yutao Zeng, Banggu Wu, Xun Zhou, and Siyuan Qiao. Ultramemv2: Memory networks scaling to 120b parameters with superior long-context learning, 2025a. URL <https://arxiv.org/abs/2508.18756>.

Zihao Huang, Qiyang Min, Hongzhi Huang, Yutao Zeng, Defa Zhu, Ran Guo, and Zhou Xun. Ultra-sparse memory network. In *ICLR*, 2025b.

Kazuki Irie, Morris Yau, and Samuel J. Gershman. Blending complementary memory systems in hybrid quadratic-linear transformers. In *NeurIPS*, 2025.

Keller Jordan, Yuchen Jin, Vlado Boza, Jiacheng You, Franz Cesista, Laker Newhouse, and Jeremy Bernstein. Muon: An optimizer for hidden layers in neural networks, 2024. URL <https://kellerjordan.github.io/posts/muon/>.

Greg Kamradt. Needle In A Haystack - Pressure Testing LLMs. https://github.com/gkamradt/LLMTest_NeedleInAHaystack, nov 2023. Accessed: 2025-12-20.

Angelos Katharopoulos, Apoorv Vyas, Nikolaos Pappas, and François Fleuret. Transformers are rnns: Fast autoregressive transformers with linear attention. In *ICML*, volume 119 of *Proceedings of Machine Learning Research*, pages 5156–5165. PMLR, 2020.

Guillaume Lample, Alexandre Sablayrolles, Marc'Aurelio Ranzato, Ludovic Denoyer, and Hervé Jégou. Large memory layers with product keys. In *NeurIPS*, 2019.

Zeman Li, Ali Behrouz, Yuan Deng, Peilin Zhong, Praneeth Kacham, Mahdi Karami, Meisam Razaviyayn, and Vahab Mirrokni. Tnt: Improving chunkwise training for test-time memorization, 2025. URL <https://arxiv.org/abs/2511.07343>.

Jessy Lin, Luke Zettlemoyer, Gargi Ghosh, Wen-Tau Yih, Aram Markosyan, Vincent-Pierre Berges, and Barlas Oğuz. Continual learning via sparse memory finetuning, 2025. URL <https://arxiv.org/abs/2510.15103>.

Calvin McCarter. Inverse distance weighting attention. In *Associative Memory & Hopfield Networks in 2023*, 2023. URL <https://openreview.net/forum?id=dHmAhYu89E>.

Amirkeivan Mohtashami and Martin Jaggi. Landmark attention: Random-access infinite context length for transformers. In *NeurIPS*, 2023.

Denis Paperno, Germán Kruszewski, Angeliki Lazaridou, Quan Ngoc Pham, Raffaella Bernardi, Sandro Pezzelle, Marco Baroni, Gemma Boleda, and Raquel Fernández. The LAMBADA dataset: Word prediction requiring a broad discourse context. In *ACL*. The Association for Computer Linguistics, 2016.

Guilherme Penedo, Hynek Kydlícek, Loubna Ben Allal, Anton Lozhkov, Margaret Mitchell, Colin A. Raffel, Leandro von Werra, and Thomas Wolf. The fineweb datasets: Decanting the web for the finest text data at scale. In *NeurIPS*, 2024.

Bo Peng, Eric Alcaide, Quentin Anthony, Alon Albalak, Samuel Arcadinho, Stella Biderman, Huanqi Cao, Xin Cheng, Michael Chung, Leon Derczynski, Xingjian Du, Matteo Grella, Kranthi Kiran GV, Xuzheng He, Haowen Hou, Przemyslaw Kazienko, Jan Kocon, Jiaming Kong, Bartłomiej Koptyra, Hayden Lau, Jiaju Lin, Krishna Sri Ipsit Mantri, Ferdinand Mom, Atsushi Saito, Guangyu Song, Xiangru Tang, Johan S. Wind, Stanislaw Wozniak, Zhenyuan Zhang, Qinghua Zhou, Jian Zhu, and Rui-Jie Zhu. RWKV: reinventing rnns for the transformer era. In Houda Bouamor, Juan Pino, and Kalika Bali, editors, *Findings of EMNLP*. Association for Computational Linguistics, 2023.

Bo Peng, Ruichong Zhang, Daniel Goldstein, Eric Alcaide, Xingjian Du, Haowen Hou, Jiaju Lin, Jiaxing Liu, Janna Lu, William Merrill, Guangyu Song, Kaifeng Tan, Saiteja Utpala, Nathan Wilce, Johan S. Wind, Tianyi Wu, Daniel Wuttke, and Christian Zhou-Zheng. RWKV-7 "goose" with expressive dynamic state evolution. In *COLM*, 2025. URL <https://openreview.net/forum?id=ayB1PA CN5j>.

Zihan Qiu, Zekun Wang, Bo Zheng, Zeyu Huang, Kaiyue Wen, Songlin Yang, Rui Men, Le Yu, Fei Huang, Suozhi Huang, Dayiheng Liu, Jingren Zhou, and Junyang Lin. Gated attention for large language models: Non-linearity, sparsity, and attention-sink-free. In *NeurIPS*, 2025. URL <https://openreview.net/forum?id=1b7wh04SfY>.

Jack W. Rae, Jonathan J. Hunt, Ivo Danihelka, Timothy Harley, Andrew W. Senior, Gregory Wayne, Alex Graves, and Tim Lillicrap. Scaling memory-augmented neural networks with sparse reads and writes. In *NeurIPS*, 2016.

Liliang Ren, Yang Liu, Yadong Lu, Yelong Shen, Chen Liang, and Weizhu Chen. Samba: Simple hybrid state space models for efficient unlimited context language modeling. In *ICLR*, 2025.

Tim Salimans and Diederik P. Kingma. Weight normalization: A simple reparameterization to accelerate training of deep neural networks. In *NeurIPS*, 2016.

Imanol Schlag, Kazuki Irie, and Jürgen Schmidhuber. Linear transformers are secretly fast weight programmers. In Marina Meila and Tong Zhang, editors, *ICML*, volume 139 of *Proceedings of Machine Learning Research*, pages 9355–9366. PMLR, 2021a.

Imanol Schlag, Tsendsuren Munkhdalai, and Jürgen Schmidhuber. Learning associative inference using fast weight memory. In *ICLR*, 2021b.

Jürgen Schmidhuber. Learning to control fast-weight memories: An alternative to dynamic recurrent networks. *Neural Comput.*, 4(1):131–139, 1992.

Noam Shazeer. Glu variants improve transformer, 2020. URL <https://arxiv.org/abs/2002.05202>.

Yu Sun, Xinhao Li, Karan Dalal, Jiarui Xu, Arjun Vikram, Genghan Zhang, Yann Dubois, Xinlei Chen, Xiaolong Wang, Sanmi Koyejo, Tatsunori Hashimoto, and Carlos Guestrin. Learning to (learn at test time): Rnns with expressive hidden states. In *ICML*, 2025.

Kimi Team, Yu Zhang, Zongyu Lin, Xingcheng Yao, Jiaxi Hu, Fanqing Meng, Chengyin Liu, Xin Men, Songlin Yang, Zhiyuan Li, Wentao Li, Enzhe Lu, Weizhou Liu, Yanru Chen, Weixin Xu, Longhui Yu, Yejie Wang, Yu Fan, Longguang Zhong, Enming Yuan, Dehao Zhang, Yizhi Zhang, T. Y. Liu, Haiming Wang, Shengjun Fang, Weiran He, Shaowei Liu, Yiwei Li, Jianlin Su, Jiezhong Qiu, Bo Pang, Junjie Yan, Zhejun Jiang, Weixiao Huang, Bohong Yin, Jiacheng You, Chu Wei, Zhengtao Wang, Chao Hong, Yutian Chen, Guanduo Chen, Yucheng Wang, Huabin Zheng, Feng Wang, Yibo Liu, Mengnan Dong, Zheng Zhang, Siyuan Pan, Wenhao Wu, Yuhao Wu, Longyu Guan, Jiawen Tao, Guohong Fu, Xinran Xu, Yuzhi Wang, Guokun Lai, Yuxin Wu, Xinyu Zhou, Zhilin Yang, and Yulun Du. Kimi linear: An expressive, efficient attention architecture, 2025. URL <https://arxiv.org/abs/2510.26692>.

Ashish Vaswani, Noam Shazeer, Niki Parmar, Jakob Uszkoreit, Llion Jones, Aidan N. Gomez, Lukasz Kaiser, and Illia Polosukhin. Attention is all you need. In *NeurIPS*, 2017.

Ke Alexander Wang, Jiaxin Shi, and Emily B. Fox. Test-time regression: a unifying framework for designing sequence models with associative memory, 2025. URL <https://arxiv.org/abs/2501.12352>.

Maurice Weber, Daniel Y. Fu, Quentin Anthony, Yonatan Oren, Shane Adams, Anton Alexandrov, Xiaozhong Lyu, Huu Nguyen, Xiaozhe Yao, Virginia Adams, Ben Athiwaratkun, Rahul Chalamala, Kezhen Chen, Max Ryabinin, Tri Dao, Percy Liang, Christopher Ré, Irina Rish, and Ce Zhang. Redpajama: an open dataset for training large language models. In *NeurIPS*, 2024.

Jason Weston, Sumit Chopra, and Antoine Bordes. Memory networks. In *ICLR*, 2015.

Songlin Yang and Yu Zhang. FLA: A triton-based library for hardware-efficient implementations of linear attention mechanism, January 2024. URL <https://github.com/fla-org/flash-linear-attention>.

Songlin Yang, Bailin Wang, Yikang Shen, Rameswar Panda, and Yoon Kim. Gated linear attention transformers with hardware-efficient training. In *ICML*, 2024a.

Songlin Yang, Bailin Wang, Yu Zhang, Yikang Shen, and Yoon Kim. Parallelizing linear transformers with the delta rule over sequence length. In *NeurIPS*, 2024b.

Songlin Yang, Jan Kautz, and Ali Hatamizadeh. Gated delta networks: Improving mamba2 with delta rule. In *ICLR*, 2025.

Jianyu Zhang and Leon Bottou. Memory mosaics at scale. In *NeurIPS*, 2025. URL <https://openreview.net/forum?id=IfD2MKTmWv>.

Jianyu Zhang, Niklas Nolte, Ranajoy Sadhukhan, Beidi Chen, and Léon Bottou. Memory mosaics. In *ICLR*, 2025a.

Tianyuan Zhang, Sai Bi, Yicong Hong, Kai Zhang, Fujun Luan, Songlin Yang, Kalyan Sunkavalli, William T. Freeman, and Hao Tan. Test-time training done right, 2025b. URL <https://arxiv.org/abs/2505.23884>.

Shu Zhong, Mingyu Xu, Tenglong Ao, and Guang Shi. Understanding transformer from the perspective of associative memory, 2025.

A. Detailed Training Settings

FwMLP To rule out the impact of implementation details unrelated to the PKM architecture, we propose a baseline model that replaces the PKM in FwPKM with a SwiGLU-MLP that maintains three fast-weight matrices (and their biases) for up, gating, and down projection. The baseline, denoted as FwMLP, updates its fast weights by minimizing the MSE loss between its predicted values and target lookahead values at a chunk level. Due to its dense nature, we reduce the MSE losses in a chunk by averaging over both sample and feature dimensions, and we do not apply the loss aggregation and gradient shaping techniques mentioned in Section 3.2.2. For the same reason, addressing optimization in Section 3.3 is irrelevant too.

LaCT We adopt the official implementation of LaCT (Zhang et al., 2025b)⁵ as a strong TTT (Sun et al., 2025) baseline. The LaCT architecture consists of a sliding window attention, a fast-weight SwiGLU MLP, and a slow-weight SwiGLU MLP in every layer. The fast weights are optimized to minimize a dot product loss via SGD with momentum or Muon (Jordan et al., 2024), and we found SGD with momentum achieves better performance in our experiments. LaCT uses data-dependent learning rate and L2 weight normalization to improve memorization and retention. One notable difference between LaCT (or more generally TTT) and FwMLP/FwPKM is that LaCT/TTT maintains an individual set of fast weights for each sequence in a mini batch, while FwMLP/FwPKM uses a shared set of fast weights for all sequences. We compared several configurations of sliding window size (W) and update chunk size (C). Among 512C + 512W, 512C + 2048W, 512C + 4096W, and 2048C + 2048W, the best model is 512C + 2048W.

Table 3 | Modeling and training hyper-parameters used in the experiments.

Hyperparameter	Value	Hyperparameter	Value	Hyperparameter	Value
<i>General</i>		<i>FwPKM</i>		<i>Training</i>	
vocab. size	32000	key dim	512	max. LR	0.001
# layers	12	value dim	512	min. LR	0.0001
hidden dim	768	# heads	1	global batch size	128
RMS norm ϵ	0.00001	Top- K	8	micro batch size	8
<i>Attention</i>		# slots	512^2	# warmup steps	100
head dim	64	chunk size	512	# total steps	20000
# query heads	12	addr. loss weight	10	weight decay	0.1
# k/v heads	4				
<i>GDN</i>		<i>FwMLP</i>			
conv. size	4	input dim	512		
head dim	64	intermediate dim	2304		
# heads	8	output dim	512		
<i>PKM</i>		LR η	0.1		
key dim	512				
value dim	512				
# heads	4				
Top- K	32				
# slots	512^2				

⁵https://github.com/a1600012888/LaCT/tree/main/lact_llm

B. Ablation Study

To understand the influence of techniques proposed in Section 3, we conduct ablation experiments based on the GDN + FwPKM@2,6,10 model. The following variants are trained and evaluated using the same pipelines.

- “w/ 1 head \times Top-32” uses a different Top- K setting as the name suggests.
- “w/ 4 heads \times Top-8” uses a different multi-head setting as the name suggests.
- “w/o value norm” does NOT z-score normalize target values.
- “w/o addr loss” does NOT use the marginal entropy loss to update key matrices, instead it uses the MSE loss to update both the keys and value matrices.
- “w/o gating” does NOT use g_t .
- “w/o loss weight” uses g_t but does NOT weight MSE loss with it.
- “w/o lookahead” does NOT use lookahead values as MSE targets.

In addition, we found that replacing IDW score with dot-product score often results in memory collapsing and loss divergence so do not include it in the ablation study.

As shown in Figures 8, 7, and 9, removing lookahead values yields the most significant harm to model performance. Many techniques bring slight PPL improvement, but lead to less healthy memory utility and subsequently worse NIAH accuracies to different extents.

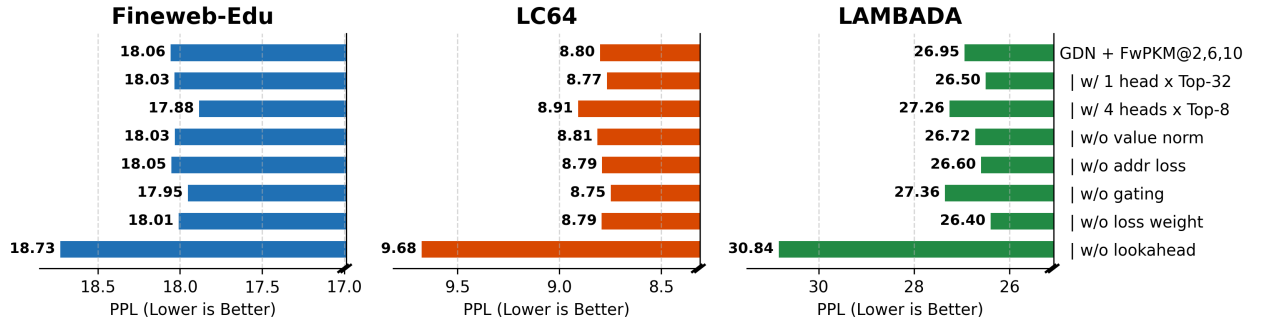


Figure 7 | Ablation study: perplexity on Fineweb-Edu, LC64, and LAMBADA

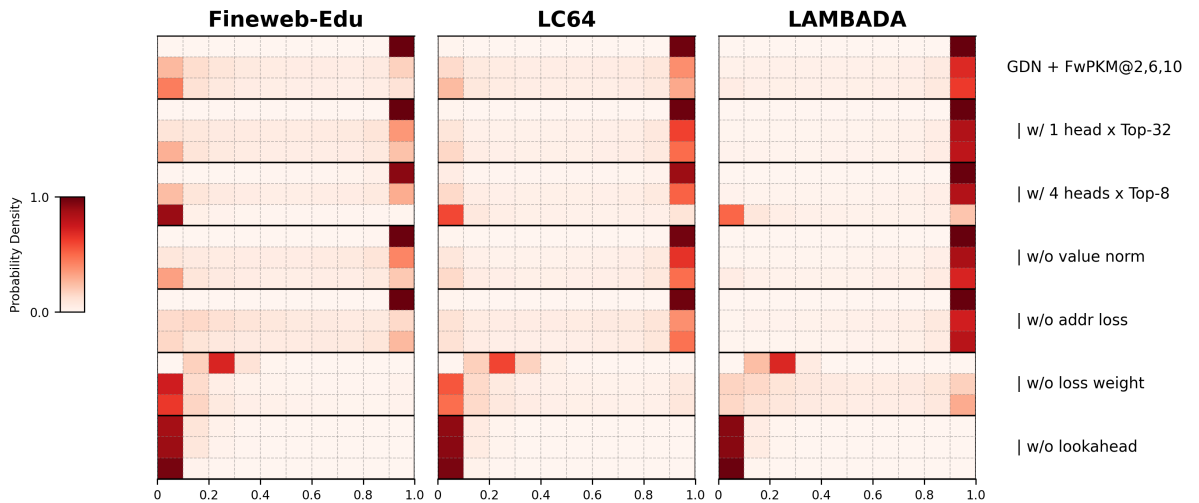


Figure 8 | Ablation study: FwPKM gating value distribution on Fineweb-Edu, LC64, and LAMBADA test sets. Each row represents one FwPKM layer.

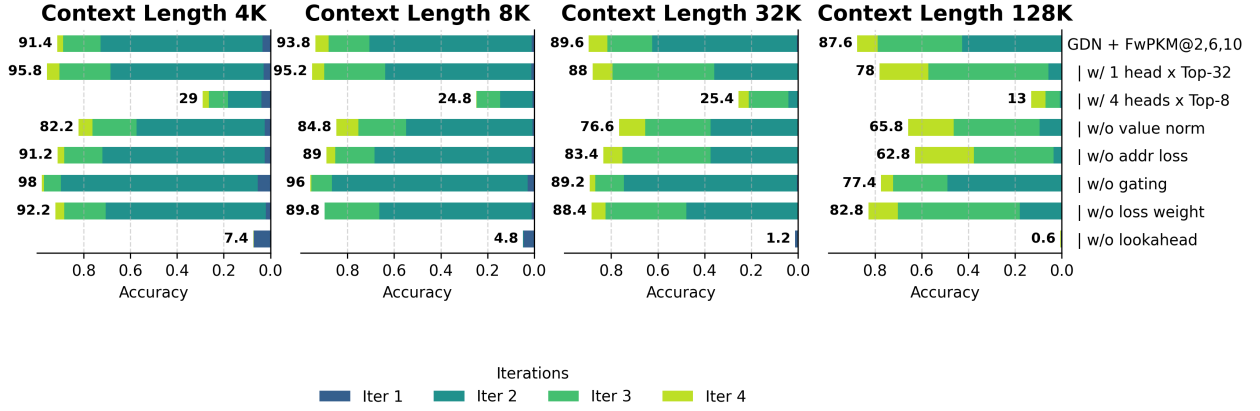


Figure 9 | Ablation study: stacked bar plots for NIAH accuracy results on 4K-/8K-/32K-/128K-length test sets. Each stacked bar shows the accuracies of {1, 2, 3, 4}-iter NIAH evaluations.

C. More Visualization Examples

Figure 10 shows the token-level FwPKM gating values for the Introduction section of this paper.

Sequence modeling layers, or token mixers, are the foundational components in modern language models. The most successful architectures today can be fundamentally understood as forms of associative memory (Dao and Gu, 2024; Peng et al., 2025; Vaswani et al., 2017; Yang et al., 2024b, 2025), characterized by their ability to maintain key-value associations, execute retrieval, and perform memorization (Gershman et al., 2025). Within this framework, existing layers exist on a spectrum defined by the trade-off between storage capacity and computational efficiency. Standard softmax attention (Vaswani et al., 2017) acts as an associative memory with unbounded storage, yet its computational cost becomes increasingly prohibitive as the sequence length grows (Zhang et al., 2025). Conversely, linear attention variants (Behrouz et al., 2025c; Dao and Gu, 2024; Gu and Dao, 2024; Katharopoulos et al., 2020; Schlag et al., 2021b; Sun et al., 2025; Yang et al., 2025) provide efficient, sub-quadratic mechanism but rely on fixed storage capacities that often struggle to capture the same depth of information.

We focus our investigation on resolving this specific tension: balancing large-scale storage with low computational overhead. We posit that an ideal associative memory should satisfy four key properties:

1. Key-value Association: The ability to link keys to values.
2. Large Storage Capacity: that is extensive, if not unbounded.
3. Low Cost: Sub-quadratic computational complexity w.r.t. input length.
4. Retrieval and Memorization: The capability to retrieve information and, crucially, memorize new key-value pairs from inputs at any time.

Product Key Memory (PKM, Lample et al., 2019) is an architecture that elegantly satisfies the first three properties. Its sparse key-value design handles an enormous number of memory slots (e.g., `<0xF0><0x9D><0x91><0x81> = 106`) with fixed and low computation. However, PKM was originally designed as a “slow-weight” channel mixer – similar to Feed-Forward Networks (FFN) – meaning it is updated only during training and remains frozen during inference. Consequently, it lacks the ability to rapidly adapt to new inputs during deployment, failing property 4.

In this paper, we propose to convert PKM from a static, slow-weight module into Fast-weight Product Key Memory (FwPKM). By redesigning PKM to update its parameters dynamically at both training and inference time, we enable it to function as a high-fidelity episodic memory. FwPKM can store “episodes” directly from input sequences and carry that memory across different contexts, offering a promising new path for continual learning and personalized AI agents.

Figure 10 | GDN+PKM@6+FwPKM@2, 10's FwPKM gating values on tokens from the Introduction section.